nanomaterials

MDPI

Article

Hot Electron Extraction in SWCNT/TiO_2 for Photocatalytic H_2 Evolution from Water

Masahiro Yamagami [1], Tomoyuki Tajima [1], Zihao Zhang [2], Jun Kano [2], Ki-ichi Yashima [3], Takana Matsubayashi [3], Huyen Khanh Nguyen [3], Naoto Nishiyama [3], Tomoya Hayashi [3] and Yutaka Takaguchi [3,*]

[1] Graduate School of Environmental and Life Science, Okayama University, 3-1-1 Tsushima-Naka, Kita-ku, Okayama 700-8530, Japan
[2] Graduate School of Natural Science and Technology, Okayama University, 3-1-1 Tsushima-naka, Kita-ku, Okayama 700-8530, Japan
[3] Department of Material Design and Engineering, Faculty of Sustainable Design, University of Toyama, Toyama 930-8555, Japan
* Correspondence: tak@sus.u-toyama.ac.jp; Tel.: +81-(0)76-445-6837

Abstract: Single-walled carbon nanotube (SWCNT)/TiO_2 hybrids were synthesized using 1,10-bis(decyloxy)decane-core PAMAM dendrimer as a molecular glue. Upon photoirradiation of a water dispersion of SWCNT/TiO_2 hybrids with visible light ($\lambda > 422$ nm), the hydrogen evolution reaction proceeded at a rate of 0.95 mmol/h·g in the presence of a sacrificial agent (1-benzyl-1,4-dihydronicotinamide, BNAH). External quantum yields (EQYs) of the hydrogen production reaction photosensitized by (6,5), (7,5), and (8,3) tubes were estimated to be 5.5%, 3.6%, and 2.2%, respectively, using monochromatic lights corresponding to their E_{22} absorptions (570 nm, 650 nm, and 680 nm). This order of EQYs (i.e., (6,5) > (7,5) > (8,3)SWCNTs) exhibited the dependence on the C_2 energy level of SWCNT for EQY and proved the hot electron extraction pathway.

Keywords: single-walled carbon nanotube; photocatalyst; hydrogen evolution; water splitting; hot electron extraction

Citation: Yamagami, M.; Tajima, T.; Zhang, Z.; Kano, J.; Yashima, K.-i.; Matsubayashi, T.; Nguyen, H.K.; Nishiyama, N.; Hayashi, T.; Takaguchi, Y. Hot Electron Extraction in SWCNT/TiO_2 for Photocatalytic H_2 Evolution from Water. *Nanomaterials* **2022**, *12*, 3826. https://doi.org/10.3390/nano12213826

Academic Editor: Antonino Gulino

Received: 6 October 2022
Accepted: 25 October 2022
Published: 29 October 2022

1. Introduction

Single-walled carbon nanotubes (SWCNTs) have attracted attention for their application as a photoelectric conversion material due to their outstanding solar light absorption property [1]. The optical absorption of semiconducting SWCNTs reveals sets of chirality-dependent absorption bands in the near-infrared and visible wavelength regions, which are labeled the first (E_{11}) and second (E_{22}) transitions, corresponding to the discrete energetic transitions of one-dimensional van Hove singularities [2]. The energy level of the second excited state (E_2 state) is higher than that of the first excited state (E_1 state). Hence, hot electron extraction directly from the E_2 state is effective to improve the performance of photovoltaics and photocatalysts based on SWCNT-light absorbers. However, regarding a SWCNT/C_{60} heterojunction, which is often used in organic solar cells, the relaxation from the E_2 state to E_1 or ground states suppresses the hot electron extraction from SWCNT to C_{60} [3]. As a result, the internal quantum efficiency (IQE) of SWCNT/C_{60} solar cells depends on an energetic offset between the lowest molecular orbital (LUMO: C_1), corresponding to the E_1 state, of the nanotube and that of C_{60} [4]. In other words, the IQE of SWCNT/C_{60} solar cells is not affected by the energy level of the E_2 state (LUMO+1: C_2) of SWCNTs, even upon E_{22} photoexcitation with visible light. Recently, we developed SWCNT/C_{60} photocatalysts that act as hydrogen evolution photocatalysts [5–9]. As in the case of SWCNT/C_{60} solar cells, the external quantum yield (EQY) of the photocatalytic hydrogen production increased in the order (7,5)SWCNT (0.17%) < (6,5)SWCNT (0.35%) < (8,3)SWCNT (1.5%) with increasing LUMO energy levels of the SWCNTs, despite photoexcitation using E_{22} absorption to generate the E_2 state [8]. Density functional theory (DFT) calculation has shown that E_{22} excitation does not induce electron injection to C_{60} in the (6,5)SWCNT/C_{60} interface, although,

with E_{11} excitation, ultrafast electron transfer (τ < 200 fs) takes place from (6,5)SWCNT to C_{60} [10]. These observations indicate that C_{60} is not capable of extracting hot electrons from SWCNTs. On the other hand, Parkinson and co-workers fabricated SWCNT heterojunctions with atomically flat surfaces of TiO_2 and SnO_2, where higher-energy second excitonic SWCNT transitions produce more photocurrent [11]. Because of the continuum of states within the metal-oxide conduction band with a density that increases with increasing energy above the conduction band minimum, rates of carrier injection from E_2 of SWCNT to TiO_2 or SnO_2 are competitive with fast hot-exciton relaxation processes. In this context, the construction of similar photocatalytic systems is of interest in order to make photocatalytic reactions using SWCNTs more efficient. In this paper, we synthesized SWCNT/TiO_2 nanohybrids to demonstrate their photocatalytic activity for hydrogen evolution from water through the hot electron extraction from the E_2 state of SWCNT to TiO_2.

2. Materials and Methods

2.1. Reagents and Chemicals

SWCNTs were purchased from Sigma-Aldrich Co (St. Louis, MO, USA). TiO_2 was synthesized according to a previous report [12]. BDD-dendrimer(COOH) [13] and SWCNT/BDD-dendrimer(COOH) [14] were prepared according to our previous reports. All other reagents were purchased from Kanto Kagaku Co., Ltd. (Tokyo, Japan), Aldrich Chemical Co. (St. Louis, MO, USA), and Tokyo Kasei Co., Ltd. (Tokyo, Japan). All chemicals were used as received.

2.2. Characterization

The absorption data were recorded on a UV-3150 spectrophotometer (Shimadzu, Tokyo, Japan) using a standard cell with a path length of 10 mm. SEM measurements for the composites were conducted using a JEM-2100 (JEOL Ltd., Tokyo, Japan). Specimens for the measurements were prepared by applying a few drops of the sample solution onto a dedicated grid, and then evaporating the solvent. Raman spectra were obtained on a JASCO NRS-5100 (JASCO Co., Japan) using laser excitation at 532 nm.

2.3. Synthesis of SWCNT/BDD-Dendrimer(COOH) Nanohybrids

SWCNT/BDD-dendrimer(COOH) nanohybrids were synthesized as follows in accordance with the literature [14]. SWCNTs (1.0 mg) were added to a solution of BDD-dendrimer(COOH) (1.0 mg, 0.13 mM) in H_2O (5.0 mL) and then sonicated using a bath-type ultrasonifier (AS ONE Vs-D100, 24 kHz/31 kHz, 110 W) at a temperature below 25 °C for 4 h. The centrifugation (3000 G) of the suspension for 30 min gave a stock solution of SWCNT/BDD-dendrimer(COOH) nanohybrids as a black-colored transparent supernatant.

2.4. Synthesis of SWCNT/TiO_2/Pt Hybrids

Here, 1.0 wt% Pt-loaded TiO_2 particles were prepared using the previously reported method [12]. The solid of TiO_2 (25 mg) was added to distilled water (22.5 mL), H_2PtCl_6 (0.66 mg, 1.28 μmol), and methanol (2.5 mL), and then irradiated by a 300 W Xe lamp (300 W, MAX-303, Asahi Spectra Co., M.C., without an optical filter) with stirring for 4 h at room temperature. After the irradiation, the gray solid was rinsed with methanol and dried under a vacuum. The SWCNTs were adsorbed onto TiO_2 by stirring the TiO_2/Pt (10 mg) in a mixture of SWCNT/BDD-dendrimer(COOH) nanohybrids (125 μL, SWCNT content 0.025 mg) in water (10 mL) at room temperature for 30 min and immersed overnight in the dark. After that, the supernatant was removed by decantation and the sample was dried and kept in the dark (denoted as SWCNT/TiO_2/Pt).

2.5. Photocatalytic Hydrogen Evolution Using SWCNT/TiO_2/Pt Hybrids

SWCNT/TiO_2/Pt (10 mg) and BNAH (38.6 mg, 180 μmol) were dissolved in deionized water (150 mL) in a Pyrex reactor. Upon vigorous stirring, the solution was irradiated with a 300 W Xenon arc light (300 W, MAX-303, Asahi Spectra Co., M.C., Tokyo, Japan)

through the cut-off filter (λ > 422 ± 5 nm: Asahi Spectra Co., M.C., 25 φ) and bandpass filter (λ = 570 nm, 650 nm, 680 nm: Asahi Spectra Co., M.C., 25 φ). After a designated period of time, the cell containing the reaction mixture was connected to a gas chromatograph (Shimadzu, TCD, molecular sieve 5 A: 2.0 m × 3.0 mm, Ar carrier gas) to measure the amount of H_2 above the solution (Figure S1).

3. Results and Discussion

Water-dispersible SWCNT/BDD-dendrimer nanohybrids were synthesized by the physical modification of SWCNTs with poly(amidoamine) dendrimer with a 1,10-bis(decyloxy)decane core and carboxy (–COOH) terminals, BDD-dendrimer(COOH) (Figure 1a) [12,13]. Pt-loaded TiO_2 mesocrystals (TiO_2/Pt) (25 mg) were prepared by a conventional photochemical deposition method [12]. The Pt loading on TiO_2 was confirmed by the hydrogen production activity (0.71 μmol/h·mg) under UV irradiation. To a water dispersion (10 mL) of TiO_2/Pt (10 mg), a solution of SWCNT/BDD-dendrimer(COOH) nanohybrids (125 μL, SWCNT content 0.025 mg) was added. The mixture was stirred for 30 min and immersed overnight in the dark. The solvent was removed by decantation to obtain SWCNT/TiO_2/Pt (Figure 1b). The amount of SWCNTs adsorbed on the TiO_2 surface was estimated to be 21 μg per 10 mg of TiO_2/Pt using the absorption spectrum of supernatant solution after the hybridization of SWCNTs with TiO_2 (Figure S2).

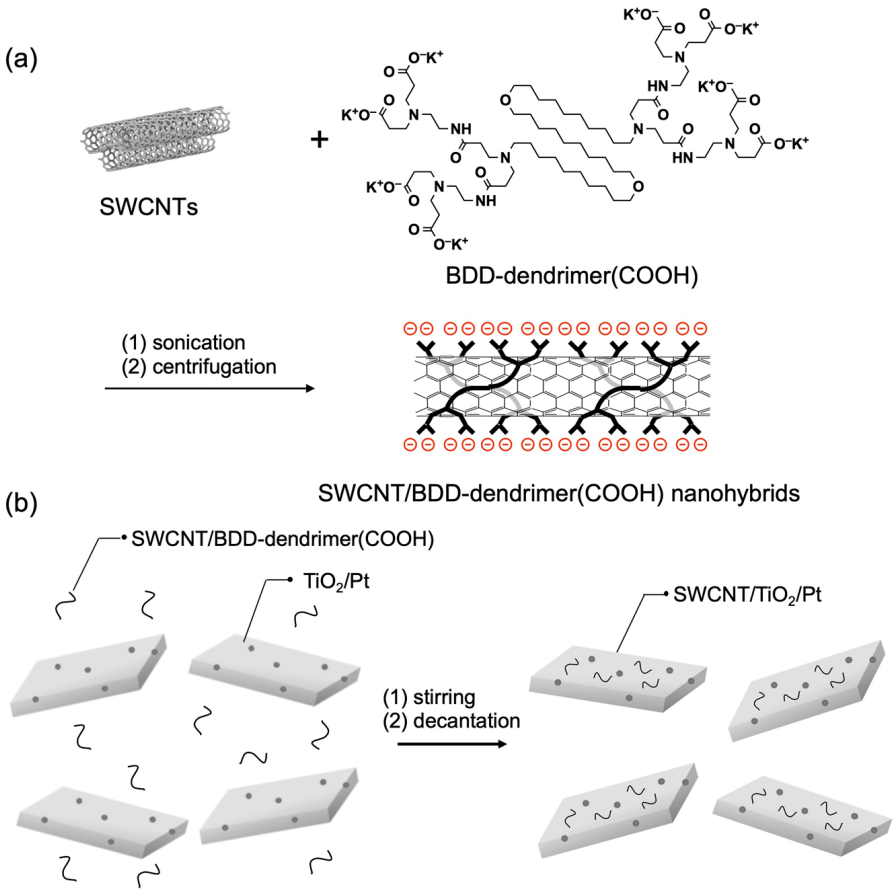

Figure 1. Fabrication of (**a**) the SWCNT/BDD-dendrimer(COOH) nanohybrids, and (**b**) SWCNT/TiO_2/Pt nanohybrids.

Figure 2 shows SEM images of TiO_2 and SWCNTs/TiO_2/Pt. The TiO_2 mesocrystals were plate-like structures with a particle size of 10 μm (Figure 2a), as previously reported [12]. The plate-like structure was retained after the attachment of SWCNT/BDD-dendrimer(COOH) nanohybrids to TiO_2 (Figure 2b). TiO_2 particles on the plate mesocrys-

tals were stripped off by ultrasonic treatment during the Pt loading or SWCNTs attachment process. Although the amount of Pt and SWCNTs on the surface of the TiO_2 crystals was so small that they could not be observed by energy dispersive X-ray spectroscopy (EDX), HR-SEM images show the Pt nanoparticles and nanofibers on the TiO_2 mesocrystals (Figure S3). The SWCNTs/TiO_2/Pt exhibited a Brunauer–Emmett–Teller (BET) surface area of 54.7 m^2 g^{-1}.

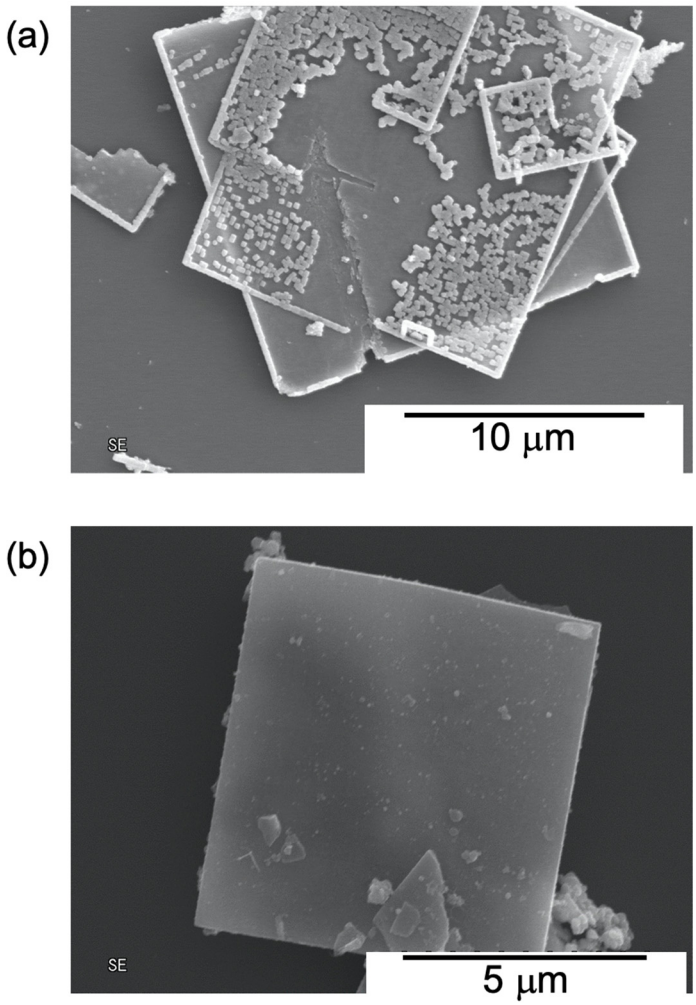

Figure 2. SEM images of (**a**) TiO_2 and (**b**) SWCNT/TiO_2/Pt.

The formation of SWCNT/TiO_2/Pt nanohybrids was confirmed by absorption, 2D excitation/emission, and Raman spectra. The absorption spectra of SWCNT/TiO_2/Pt (blue line) exhibit the characteristic absorption bands derived from SWCNTs that appeared at 400–700 nm (Figure 3). The absorption originating from (6,5)SWCNT (λ_{max} 570 nm) along with a small shoulder at around 670 nm originating from (8,3) and (7,5)SWCNTs were observed, almost the same as that of SWCNT/BDD-dendrimer(COOH) (orange line). Two-dimensional excitation/emission spectra show the quenching of the fluorescence of SWCNTs after the hybridization with TiO_2/Pt due to photoinduced electron transfer from SWCNTs to TiO_2 (Figure S4).

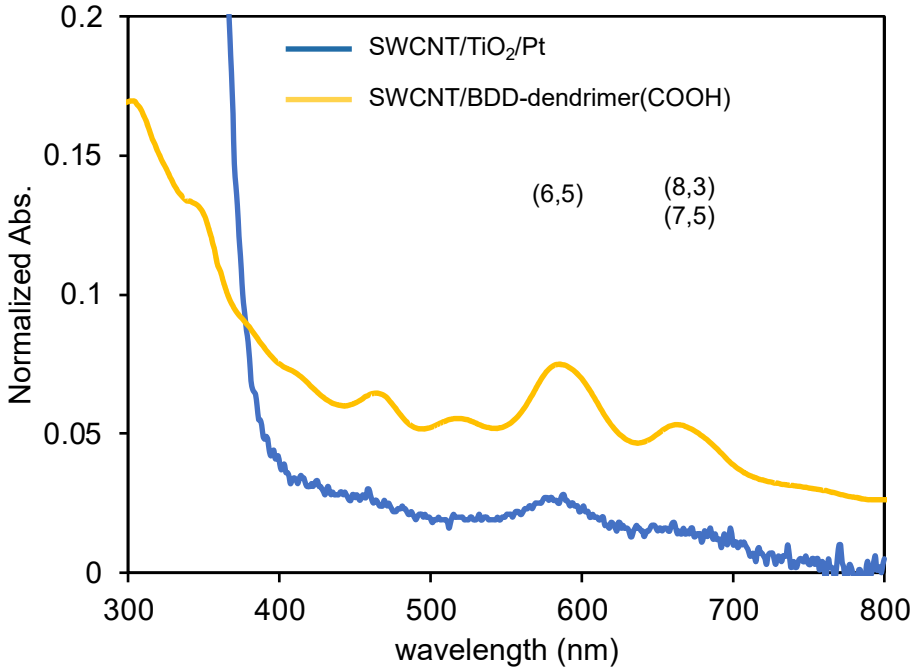

Figure 3. Absorption spectra of SWCNT/TiO_2/Pt (blue line) and SWCNT/BDD-dendrimer(COOH) nanohybrids (orange line).

Figure 4 shows the Raman spectrum of the SWCNT/TiO_2/Pt hybrids. Raman shifts for the G band (1585 cm^{-1}), D band (1316 cm^{-1}), and G′ band (2622 cm^{-1}) of the SWCNTs were observed, where the G/D ratio (3.30) did not change before or after the attachment of SWCNT onto TiO_2, indicating that the sp^2 carbon of SWCNTs was not changed to sp^3 carbon. Peaks originating from the anatase crystal of TiO_2 were observed at 403 cm^{-1} (B_{1g}), 517 cm^{-1} (A_{1g}), 156 cm^{-1}, and 643 cm^{-1} (E_g) [15]. These observations indicate that SWCNTs are adsorbed on the surface of TiO_2.

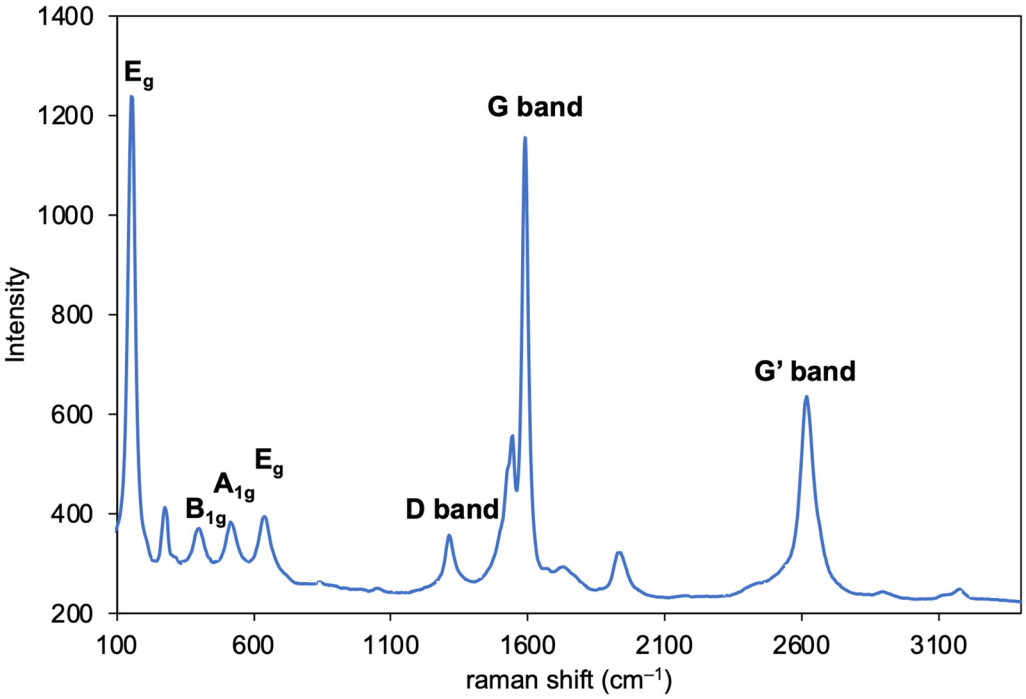

Figure 4. Raman spectrum of SWCNT/TiO_2/Pt hybrids.

Parkinson and co-workers reported that hot electron injection from the SWCNT E_{22} state to TiO_2 is more efficient than electron injection from the relaxed SWCNT E_{11} state at the SWCNT/TiO_2 heterojunction due to a higher density of states (DOS) at E_{22} than at E_{11} of SWCNTs and the continuum of states within the TiO_2 conduction band with a density that increases with increasing energy above the conduction band edge [11]. In marked contrast with SWCNT/C_{60} heterojunctions [3,10], hot electron extraction from the SWCNT E_{22} state (C_2) is fast enough to compete with relaxation to the E_{11} state (C_1) so that the relative photon conversion efficiency (RPCE) upon E_{22} photoexcitation is higher than that upon E_{11} photoexcitation. In this context, we expected photocatalytic hydrogen evolution from water using SWCNT/TiO_2/Pt nanohybrids via direct electron extraction from SWCNT E_{22} states (C_2), of which the energy level diagram is shown in Figure 5. Higher-energy second excitonic SWCNT transition under visible-light irradiation leads to hot electron extraction from the SWCNT E_{22} state (C_2) to the TiO_2 conduction band, followed by the electron migration to the Pt co-catalyst to induce the hydrogen evolution reaction. The remaining hole in the SWCNT valence bands (V_2) is consumed by simultaneous hole migration to a sacrificial donor molecule, 1-benzyl-1,4-dihydronicotinamide (BNAH). The efficiency of the hydrogen evolution reaction is dominated by the efficiency of the hot electron extraction from SWCNT E_{22} to TiO_2, because the electron injection from the SWCNT E_{11} state (C_1) to TiO_2 is relatively slow due to the small driving forces, although the hot-electron injection rate from C_2 to TiO_2 is competitive with hot-exciton relaxation processes, as described by Parkinson et al. [11].

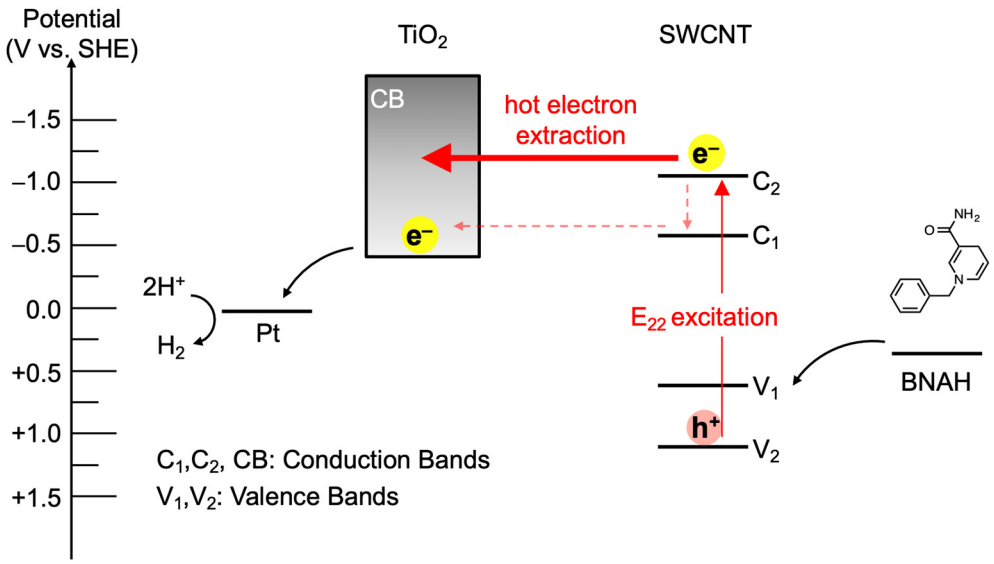

Figure 5. Energy-level diagram of the hydrogen evolution reaction using SWCNT/TiO_2/Pt as a photocatalyst in the presence of BNAH as a sacrificial donor.

Figure 6 shows the time course of the photocatalytic hydrogen evolution reaction over SWCNT/TiO_2/Pt under visible-light irradiation ($\lambda > 422$ nm). The hydrogen production rate of 9.5 μmol/h was observed (Figure 6, ●). The hydrogen evolution reaction continued until all of the sacrificial agent, BNAH, was consumed, and there was no induction period (Figure S5). In contrast, no production of hydrogen was detected using TiO_2/Pt without SWCNTs under the same conditions (Figure 6, ■), indicating that the SWCNTs act as photosensitizers and the hydrogen production reaction proceeds via electron extraction from SWCNTs on the surface of TiO_2. To compare the electron-extracting ability of TiO_2, commercially available P25 was used to synthesize SWCNT/TiO_2(P25)/Pt. Under the same reaction conditions, the hydrogen production rate of SWCNT/TiO_2(P25)/Pt was 7.3 μmol/h (Figure S6), which is less active than that of SWCNT/TiO_2(mesocrystal)/Pt (9.5 μmol/h). The higher activity with TiO_2 mesocrystals may be due to the suppres-

sion of charge recombination at the SWCNT/TiO_2 interface. A similar result using black phosphorous/TiO_2 (mesocrystal) interface was described by Fujitsuka and co-workers [16].

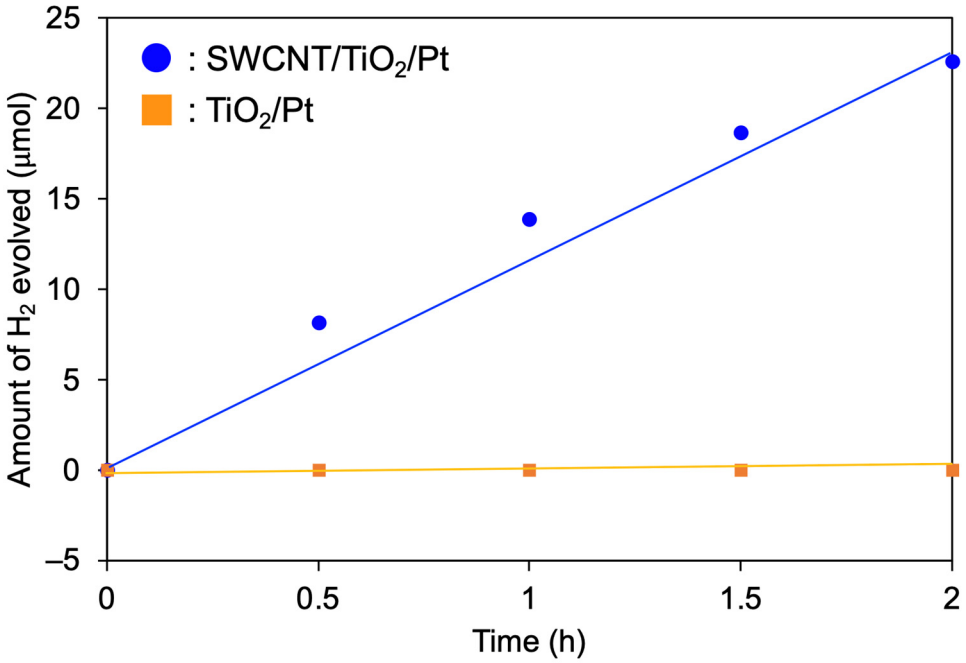

Figure 6. Time course of H_2 evolution from water over SWCNT/TiO_2/Pt (blue line) and TiO_2/Pt (orange line) under visible-light irradiation (λ > 422 nm).

To obtain insight into this free-carrier generation process in the SWCNT/TiO_2 heterojunction, we compared the chirality dependence of EQY of the hydrogen evolution reaction using the SWCNT/TiO_2 heterojunction with that using SWCNT/C_{60} upon E_{22} photoexcitation of SWCNTs. In our previous reports [8,9], we found a commensurate reduction of EQY in the offset of the energy levels (driving force) between SWCNT C_1 and C_{60} LUMO (Figure 7). (8,3)SWCNT shows the highest EQY among (6,5), (7,5), and (8,3)SWCNTs because of the electron transfer from SWCNT to C_{60} after the relaxation from the SWCNT E_{22} state to the SWCNT E_{11} state, as in the case of SWCNT/C_{60} solar cells. If the hot electron extraction from the SWCNT E_{22} state to C_{60} had occurred, the EQY would depend on the energy levels of SWCNT C_2, i.e., (6,5)SWCNT would represent the highest EQY, and (8,3)SWCNT would show the lowest EQY.

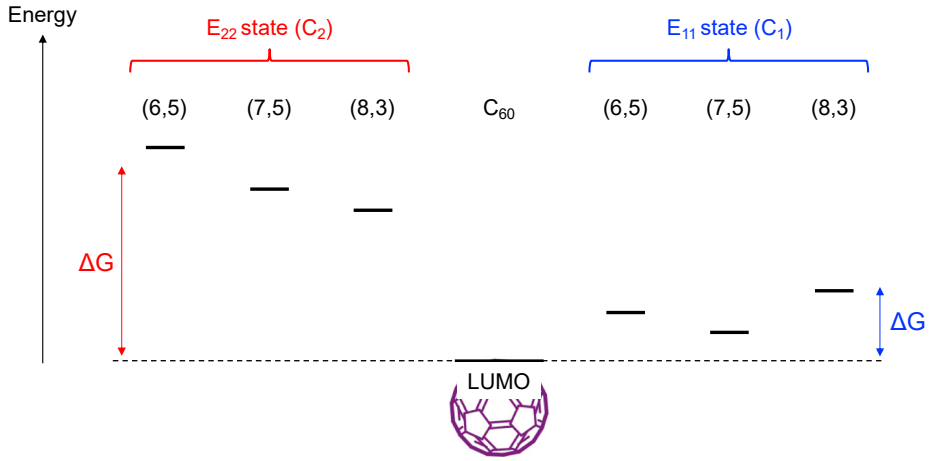

Figure 7. Driving force of electron extraction using SWCNT/C_{60} heterojunction from SWCNT E_{22} state (**left** side) and SWCNT E_{11} state (**right** side).

In this context, we investigated the photocatalytic activity of SWCNT/TiO_2/Pt upon chirality-selective photoexcitation using monochromatic light irradiation at 570, 650, and 680 nm, which are the E_{22} absorptions of (6,5), (7,5), and (8,3)SWCNTs, respectively. In a typical experiment, 150 mL of an aqueous dispersion of SWCNT/TiO_2/Pt (10 mg) and 1-benzyl-4-dihydronicotinamide (BNAH; 38.6 mg, 180 μmol/h) was exposed to monochromatic light (570, 650, or 680 nm) using a 300 W Xenon arc lamp with bandpass filters while being stirred vigorously at 25 °C. After the designated period, the gas phase above the solution was analyzed by gas chromatography. Figure 8a (●) shows plots of the total amount of H_2 produced versus time using monochromatic light irradiation at 570 nm. A steady generation of H_2 (2.2 μmol/h) was observed without an induction period or a decrease in activity during 3 h of irradiation. Compared with the H_2 generated by the use of monochromatic light irradiation at 650 or 680 nm, 1.7 μmol/h (Figure 8a (■)) and 1.3 μmol/h (Figure 8a (◆)), respectively, the amount of H_2 evolution under 570 nm irradiation was the highest (2.2 μmol/h, Figure 8a (●)). The EQYs were in the same order as for the hydrogen production rate: 5.5% for (6,5)SWCNT > 3.6% for (7,5)SWCNT > 2.2% for (8,3)SWCNT. Notably, this order of EQYs is consistent with the energy levels of the second excitonic state (C_2) for (6,5), (7,5), and (8,3)SWCNTs, –3.30, –3.54, and –3.62 eV, respectively (Figure 9), and is the same as previous reports on the relative photon conversion efficiency (RPCE) of the SWCNT/TiO_2 heterojunction. This result indicated that the hot electron injection from the second excitonic state of SWCNTs to TiO_2 leads to a hydrogen evolution reaction in marked contrast to CNT photocatalyst based on the SWCNT/C_{60} heterojunction, where the electron extraction from SWCNT to C_{60} occurred after the inter-band transition from the E_{22} state (C_2) to the E_{11} state (C_1). Furthermore, the SWCNT/TiO_2/Pt photocatalyst exhibited higher EQYs than the previously reported SWCNT/C_{60}/Pt(II) photocatalyst. For example, upon 570 nm photoirradiation (E_{22} absorption of (6,5)SWCNT), the EQY of SWCNT/TiO_2/Pt, 5.5%, is 16 times higher than that of SWCNT/C_{60}/Pt(II), 0.35%.

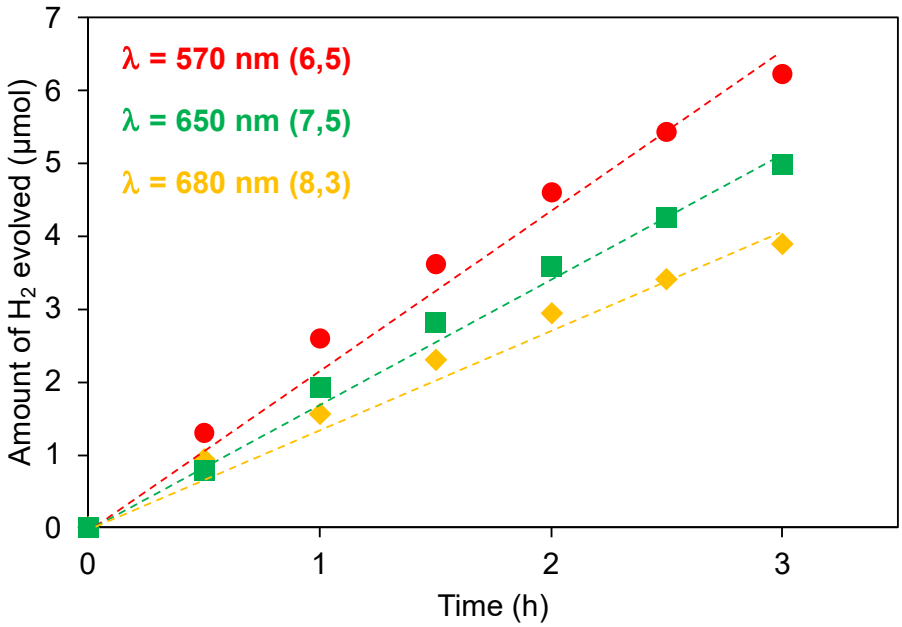

Figure 8. Time course of the H_2 evolution under irradiation at 570 nm (E_{22} of the (6,5)SWCNT; ●), 650 nm (E_{22} of (7,5)SWCNT; ■), and 680 nm (E_{22} of the (8,3)SWCNT; ▲).

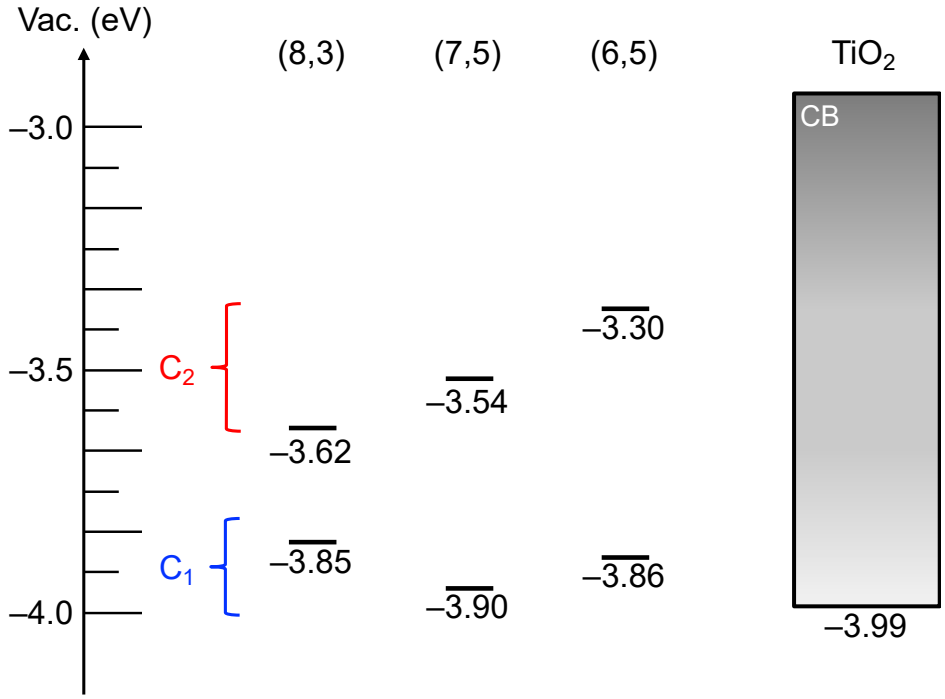

Figure 9. Energy level diagram of SWCNT/TiO_2 heterojunctions. Gray bar reveals the conduction band of TiO_2.

4. Conclusions

In summary, we have prepared a visible-light-responsive TiO_2 photocatalyst, SWCNT/TiO_2/Pt, by mixing TiO_2/Pt and SWCNT/BDD-dendrimer nanohybrids. Since BDD-dendrimer can act as a molecular glue that does not suppress the electron transfer between SWCNT and TiO_2, the photoinduced electron transfer from SWCNT to TiO_2 proceeds very smoothly to form a charge-separated state (SWCNT$^+$/TiO_2^-). The dependence on the C_2 energy level of SWCNT for the EQY of the hydrogen evolution reaction upon E_{22} photoexcitation proved the hot electron extraction pathway. Interestingly, the EQYs are higher than those of the previous reports employing SWCNT/C_{60}/Pt(II) as a photocatalyst because of the difference in the charge collection process where electron extraction takes place after the relaxation from the SWCNT E_{22} state to the SWCNT E_{11} state. Further studies on the SWCNT heterojunction with metal oxides to enhance the efficiency of the hot electron extraction pathway for solar hydrogen production are currently in progress in our laboratories.

Supplementary Materials: The following supporting information can be downloaded at: https://www.mdpi.com/article/10.3390/nano12213826/s1, Figure S1: Photograph of closed circulation system used in a photocatalytic hydrogen evolution reaction; Figure S2: Absorption spectra of supernatant before/after the hybridization of SWCNTs with TiO_2; Figure S3: HR-SEM images of SWCNT/TiO_2/Pt using in-lens detector; Figure S4: Two-dimensional PL intensity maps of (a) SWCNT/BDD-dendrimer(COOH) nanohybrids and (b) SWCNT/TiO_2/Pt; Figure S5: A time course of photocatalytic hydrogen evolution using SWCNT/TiO_2/Pt under visible light irradiation ($\lambda > 422$ nm); Figure S6: A time course of H_2 evolution from water over SWCNT/TiO_2(P25)/Pt under visible light irradiation ($\lambda > 422$ nm).

Author Contributions: Conceptualization, M.Y. and Y.T.; validation, M.Y.; formal analysis, Y.T.; investigation, M.Y., K.-i.Y., T.M. and H.K.N.; resources, Z.Z. and J.K.; data curation, T.T., N.N. and T.H.; writing—original draft preparation, M.Y; writing—review and editing, Y.T.; visualization, M.Y.; supervision, Y.T.; project administration, Y.T.; funding acquisition, N.N. and Y.T. All authors have read and agreed to the published version of the manuscript.

Funding: This research received no external funding.

Institutional Review Board Statement: Not applicable.

Informed Consent Statement: Not applicable.

Data Availability Statement: The data presented in this study are available on request from the corresponding author.

Conflicts of Interest: The authors declare no conflict of interest.

References

1. Blackburn, J.L. Semiconducting Single-Walled Carbon Nanotubes in Solar Energy Harvesting. *ACS Energy Lett.* **2017**, *2*, 1598–1613. [CrossRef]
2. Kim, P.; Odom, T.W.; Huang, J.-L.; Lieber, C.M. Electronic Density of States of Atomically Resolved Single-Walled Carbon Nanotubes: Van Hove Singularities and End States. *Phys. Rev. Lett.* **1999**, *82*, 1225–1228. [CrossRef]
3. Bindl, D.J.; Arnold, M.S. Efficient Exciton Relaxation and Charge Generation in Nearly Monochiral (7, 5) Carbon Nanotube/C_{60} Thin-Film Photovoltaics. *J. Phys. Chem. C* **2013**, *117*, 2390–2395. [CrossRef]
4. Pfohl, M.; Glaser, K.; Graf, A.; Mertens, A.; Tune, D.D.; Puerckhauer, T.; Alam, A.; Wei, L.; Chen, Y.; Zaumseil, J.; et al. Probing the Diameter Limit of Single Walled Carbon Nanotubes in SWCNT: Fullerene Solar Cells. *Adv. Energy Mater.* **2016**, *6*, 1600890. [CrossRef]
5. Tajima, T.; Sakata, W.; Wada, T.; Tsutsui, A.; Nishimoto, S.; Miyake, M.; Takaguchi, Y. Photosensitized Hydrogen Evolution from Water Using a Single-Walled Carbon Nanotube/Fullerodendron/SiO_2 Coaxial Nanohybrid. *Adv. Mater.* **2011**, *23*, 5750–5754. [CrossRef]
6. Sasada, Y.; Tajima, T.; Wada, T.; Uchida, T.; Nishi, M.; Ohkubo, T.; Takaguchi, Y. Photosensitized Hydrogen Evolution from Water Using Single-Walled Carbon Nanotube/Fullerodendron/Pt(II) Coaxial Nanohybrids. *New J. Chem.* **2013**, *37*, 4214–4219. [CrossRef]
7. Kurniawan, K.; Tajima, T.; Kubo, Y.; Miyake, H.; Kurashige, W.; Negishi, Y.; Takaguchi, Y. Incorporating a TiO_x Shell in Single-Walled Carbon Nanotube/Fullerodendron Coaxial Nanowires: Increasing the Photocatalytic Evolution of H_2 from Water under Irradiation with Visible Light. *RSC Adv.* **2017**, *7*, 31767–31770. [CrossRef]
8. Murakami, N.; Tango, Y.; Miyake, H.; Tajima, T.; Nishina, Y.; Kurashige, W.; Negishi, Y.; Takaguchi, Y. SWCNT Photocatalyst for Hydrogen Production from Water upon Photoexcitation of (8, 3) SWCNT at 680-nm Light. *Sci. Rep.* **2017**, *7*, 43445. [CrossRef] [PubMed]
9. Izawa, T.; Kalousek, V.; Miyamoto, D.; Murakami, N.; Miyake, H.; Tajima, T.; Kurashige, W.; Negishi, Y.; Ikeue, K.; Ohkubo, T.; et al. Carbon-Nanotube-Based Photocatalysts for Water Splitting in Cooperation with $BiVO_4$ and $[Co(Bpy)_3]^{3+/2+}$. *Chem. Lett.* **2019**, *48*, 410–413. [CrossRef]
10. Yang, J.J.; Li, Z.W.; Liu, X.Y.; Fang, W.H.; Cui, G. Photoinduced Electron Transfer from Carbon Nanotubes to Fullerenes: C_{60} Versus C_{70}. *Phys. Chem. Chem. Phys.* **2020**, *22*, 19542–19548. [CrossRef] [PubMed]
11. Kubie, L.; Watkins, K.J.; Ihly, R.; Wladkowski, H.V.; Blackburn, J.L.; Rice, W.D.; Parkinson, B.A. Optically Generated Free-Carrier Collection from an All Single-Walled Carbon Nanotube Active Layer. *J. Phys. Chem. Lett.* **2018**, *9*, 4841–4847. [CrossRef] [PubMed]
12. Bian, Z.; Tachikawa, T.; Kim, W.; Choi, W.; Majima, T. Superior Electron Transport and Photocatalytic Abilities of Metal-Nanoparticle-Loaded TiO_2 Superstructures. *J. Phys. Chem. C* **2012**, *116*, 25444–25453. [CrossRef]
13. Nishimura, S.; Tajima, T.; Hasegawa, T.; Tanaka, T.; Takaguchi, Y.; Oaki, Y.; Imai, H. Synthesis of Poly(Amidoamine) Dendrimer Having a 1,10-Bis(Decyloxy)Decane Core and Its Use in Fabrication of Carbon Nanotube/Calcium Carbonate Hybrids through Biomimetic Mineralization. *Can. J. Chem.* **2017**, *95*, 935–941. [CrossRef]
14. Ishimoto, K.; Tajima, T.; Miyake, H.; Yamagami, M.; Kurashige, W.; Negishi, Y.; Takaguchi, Y. Photo-Induced H_2 Evolution from Water: Via the Dissociation of Excitons in Water-Dispersible Single-Walled Carbon Nanotube Sensitizers. *Chem. Commun.* **2018**, *54*, 393–396. [CrossRef] [PubMed]
15. Ohsaka, T.; Izumi, F.; Fujiki, Y. Raman Spectrum of Anatase, TiO_2. *J. Raman Spectrosc.* **1978**, *7*, 321–324. [CrossRef]
16. Elbanna, O.; Zhu, M.; Fujitsuka, M.; Majima, T. Black Phosphorus Sensitized TiO_2 Mesocrystal Photocatalyst for Hydrogen Evolution with Visible and Near-Infrared Light Irradiation. *ACS Catal.* **2019**, *9*, 3618–3626. [CrossRef]